Sr–Nd isotope evidence for modern aeolian dust sources in mountain glaciers of western China

Jianzhong XU,[1] Guangming YU,[1] Shichang KANG,[2] Shugui HOU,[1,3] Qianggong ZHANG,[2] Jiawen REN,[1] Dahe QIN[1]

[1]*State Key Laboratory of Cryospheric Sciences, Cold and Arid Regions Environmental and Engineering Research Institute, Chinese Academy of Sciences, Lanzhou, China*
E-mail: jzxu@lzb.ac.cn
[2]*Institute of Tibetan Plateau Research, Chinese Academy of Sciences, Beijing, China*
[3]*MOE, Key Laboratory for Coast and Island Development, School of Geographic and Oceanographic Sciences, Nanjing University, Nanjing, China*

ABSTRACT. In order to apportion the dust sources of mountain glaciers in western China, the Sr–Nd isotopic compositions of insoluble particles were determined in snow samples collected from 13 sites. The combined plot of $^{87}Sr/^{86}Sr$ and $\varepsilon_{Nd}(0)$ demonstrates a distinctive geographic pattern over western China, which can be classified into three regions from north to south. Samples from the Altai mountains show the lowest $^{87}Sr/^{86}Sr$ ratio and the highest $\varepsilon_{Nd}(0)$ value, similar to the data of deserts in the north of China such as the Gurbantunggut desert. Samples from the southern Tibetan Plateau (TP) and Himalaya show the highest $^{87}Sr/^{86}Sr$ and lowest $\varepsilon_{Nd}(0)$ values, resembling the local and regional dust sources found in the southern TP and Himalaya–India region. Samples from the Tien Shan and northern Tibetan Plateau exhibit intermediate $^{87}Sr/^{86}Sr$ and $\varepsilon_{Nd}(0)$ values, similar to the data reported for the northern margin of the TP (NM_TP). However, three sampling sites, JMYZ (Jiemayangzong) located in the Himalaya and ZD (Zadang) and YL (Yulong) located in the southeast TP, presented distinctive Sr–Nd isotopic signatures typical of the NM_TP, suggesting potential long-range and high-altitude dust transport across the TP.

1. INTRODUCTION

Glaciers in the mountains of western China are unique recording media of paleoclimate and paleoenvironment in mid-latitudes (e.g. Thompson and others, 2000). Based on particle concentrations in ice cores, researchers can back-calculate the historical aerosol loadings and composition, which reflect environmental change, such as historical dust-storm frequencies (Xu and others, 2007), extreme drought events (Thompson and others, 2000) and anthropogenic impacts (Hong and others, 2009; Kaspari and others, 2011) in the source area. Yet the connection between dust sources and sinks remains uncertain. For example, there is little knowledge of how dust gets lost and is altered during and after transportation. In the past decade, isotopic and geochemical methods have been developed to address these uncertainties. The strontium–neodymium (Sr–Nd) isotopic composition was found to be particularly important as different source materials have unique profiles reflecting their origins and ages, and these profiles undergo little change during weathering, transportation and deposition (Biscaye and others, 1997; Grousset and Biscaye, 2005; Bory and others, 2010).

Arid and semi-arid areas in Central Asia including the Taklimakan, Gobi and Thar deserts make up the second largest dust source on Earth. There has been increasing focus on the dust transportation and deposition from these areas due to the large amount of emitted dust and its significant climatic and environmental impacts (Duce and others, 1980; Huang and others, 2010). For instance, there is growing concern regarding dust emission due to its effect on glacier melting and alteration of biogeochemical cycles (Fujita, 2007); however, available datasets in these areas remain limited to the identification and distinguishing of dust sources. The Sr–Nd isotopic method has only been applied at a few sites in the mountain glaciers of these areas to trace the dust sources (Xu and others, 2009; G. Wu and others, 2010). The goal of this study is to characterize the dust sources and investigate the transport of dust in these areas utilizing a more comprehensive Sr–Nd isotopic dataset.

2. SAMPLING SITES AND METHODS

Between September 2008 and November 2010, 15 snow pits were collected from 13 mountain glaciers in western China (Fig. 1). Table 1 presents the details of sampling location, collection time and snow-pit depth. At each sampling site, snow samples were collected from the snow pit at a vertical resolution of 5–20 cm, following the clean-hands-and-dirty-hands protocol with sampling personnel wearing integral Tyvek® bodysuits, non-powdered gloves and masks to avoid possible contamination (Fitzgerald, 1999). All sampling sites except Yala were chosen from the accumulation area of glaciers, and most snow pits have accumulated for more than 1 year (Zhang and others, 2012). The Yala samples were collected from the terminus of a glacier due to its harsh condition. Insoluble particles in the snow samples for each research site were obtained by centrifugation (15 000 rpm) and heating evaporation. After each centrifugation cycle (30 min), the supernatant was discarded using a syringe, and the remaining water (~10 mL) was evaporated in a class 100 laminar flow box.

Extracted particles were dissolved in an $HF–HClO_4$ mixture, and kept at 100–120°C for 7 days. Taking into account the low quantity of the samples, the Sr–Nd separation and purification were carried out following the low-background method. Briefly, rubidium (Rb)–Sr and light

https://doi.org/10.3189/2012JoG12J006 Published online by Cambridge University Press

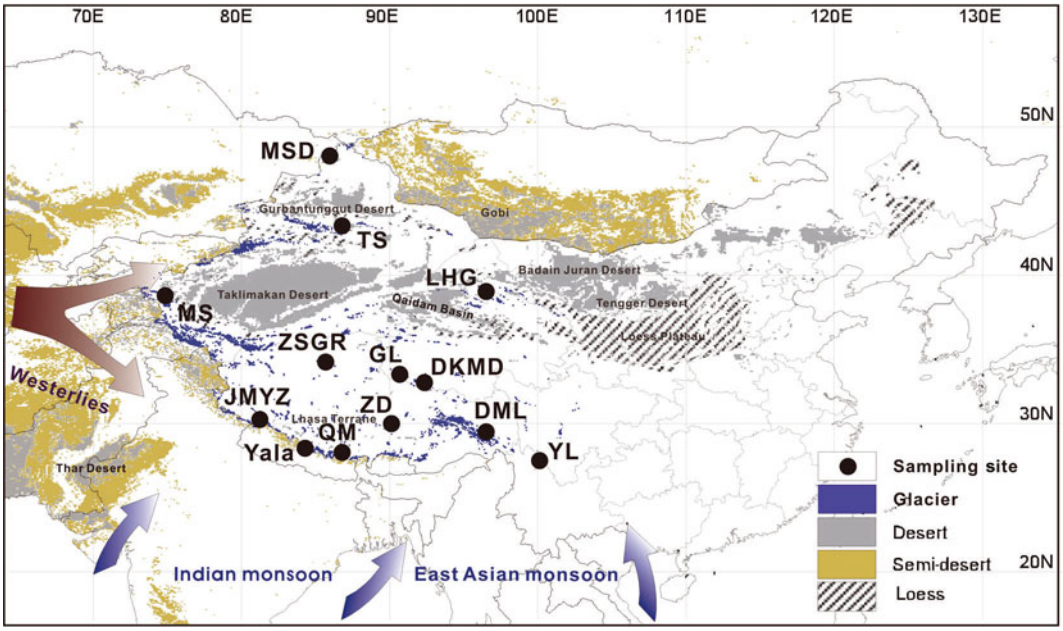

Fig. 1. Location map of snow samples collected from western China between 2008 and 2010. The distribution of dust sources and general weather patterns in winter (blue) and summer (red) circulation systems are also shown.

rare-earth elements were isolated on quartz columns by conventional ion-exchange chromatography with a 5 mL resin bed of AG 50 W-X12 (200–400 mesh) after sample decomposition. Nd and samarium (Sm) were separated from the other rare-earth elements on quartz columns using 1.7 mL of Teflon powder coated with di (2-ethylhexyl) orthophosphoric acid (HDEHP) as the cation exchange medium. Sr–Nd isotopic data were acquired using a Finnigan MAT-262 mass spectrometer (Thermo Scientific, Waltham, MA, USA). The $^{87}Sr/^{86}Sr$ and $^{143}Nd/^{144}Nd$ ratios were corrected for mass fractionation relative to $^{86}Sr/^{88}Sr = 0.1194$ and $^{146}Nd/^{144}Nd = 0.7219$, respectively (all errors were kept at 2σ) (Table 2). Meanwhile, five independent runs of standard Ames metal solutions and NBS987 yielded mean values of 0.51244 ± 0.000018 for the $^{143}Nd/^{144}Nd$ ratio and 0.710246 ± 0.000021 for the $^{87}Sr/^{86}Sr$ ratio. The maximum values of blank samples were <0.1 ng for both Sr and Nd. For convenience, the $^{143}Nd/^{144}Nd$ ratios were normalized and denoted as $\varepsilon_{Nd}(0) = [(^{143}Nd/^{144}Nd)/0.512638 - 1] \times 10^4$.

3. RESULTS AND DISCUSSION

3.1. Sr–Nd isotopic composition

The Sr and Nd isotopic compositions show large and structured variations ranging from 0.713 to 0.753 in $^{87}Sr/^{86}Sr$, and –4.8 to –16.3 in $\varepsilon_{Nd}(0)$ (Table 2). Overall, the Sr–Nd isotopic compositions reveal a strong geographic trend in western China, with high-$\varepsilon_{Nd}(0)$–low-$^{87}Sr/^{86}Sr$ signature in the north and low-$\varepsilon_{Nd}(0)$–high-$^{87}Sr/^{86}Sr$ signature in the south (Fig. 2). The MSD sample collected from the Altai mountains shows the highest $\varepsilon_{Nd}(0)$ and lowest $^{87}Sr/^{86}Sr$ values of all the samples, similar to values from the north of

Table 1. Summary of the sampling location, time and snow-pit depth at each site in western China

Site name	Glacier	Area	Location	Sampling date	Altitude m a.s.l.	Depth cm
MSD	Musidao	Altai mountains	47.01° N, 85.55° E	27 Aug 2010	3605	120
TS	Glacier No. 1	Tien Shan	43.11° N, 86.81° E	20 Oct 2008	4063	220
MS	Muztagata	East Pamirs	38.28° N, 75.01° E	28 Jul 2009	6365	150
LHG1	Laohugou No.12	Qilian mountains	39.43° N, 96.56° E	16 Oct 2008	5026	130
LHG2				28 Oct 2009	5026	100
ZSGR	Zangsegangri	Qiangtang plateau	34.3° N, 85.85° E	3 May 2009	6226	101
DKMD	Dongkemadi	Tanggula mountains	33.01° N, 92.01° E	15 May 2009	5700	20
GL	Guoqu	Tanggula mountains	33.58° N, 91.18° E	23 Apr 2009	5765	74
JMYZ	Jiemayangzong	Himalaya	30.21° N, 91.18° E	4 June 2009	5558	188
Yala	Yala	Himalaya	28.23° N, 91.18° E	26 Oct 2010	5190	20
QM	East Rongbuk	Himalaya	28.01° N, 86.97° E	18 May 2009	6525	115
ZD1	Zadang	Nyainqentanglha	30.47° N, 90.65° E	16 Sep 2008	5758	200
ZD2				7 May 2009	5797	210
DML	Demula	Hengduan mountains	29.37° N, 97.00° E	21 Sep 2008	5404	180
YL	Baishui No. 1	Hengduan mountains	27.1° N, 100.2° E	20 May 2009	4747	295

https://doi.org/10.3189/2012JoG12J006 Published online by Cambridge University Press

Table 2. Sr–Nd isotopic composition of snow samples from mountain glaciers of western China. NA: no data available

Sample	Location	$^{87}Sr/^{86}Sr$	Error (2σ)	$^{143}Nd/^{144}Nd$	Error (2σ)	$\varepsilon_{Nd}(0)$
MSD-1	47.01° N, 85.55° E	0.713268	0.000022	0.512392	0.000020	–4.8
MSD-2		0.713571	0.000019	0.512302	0.000024	–6.55
MSD-3		0.713185	0.000033	0.512358	0.000060	–5.46
TS-1	43.11° N, 86.81° E	0.719926	0.000055	0.512207	0.000063	–8.41
TS-2		0.720722	0.000047	NA	NA	NA
TS-3		0.721728	0.000024	NA	NA	NA
TS-4		0.719005	0.000024	NA	NA	NA
TS-5		0.719802	0.000018	0.512286	0.000052	–6.87
TS-6		0.720716	0.000037	0.512212	0.000133	–8.31
TS-7		0.719404	0.000013	0.512267	0.000055	–7.24
MS-1	38.28° N, 75.01° E	0.717187	0.000028	0.512163	0.000231	–9.27
MS-2		0.717248	0.000023	0.512206	0.000013	–8.43
MS-3		0.717415	0.000013	0.512111	0.000037	–10.28
LHG-1	39.43° N, 96.56° E	0.720448	0.000017	0.511852	0.000014	–15.33
LHG-2		0.720699	0.000018	0.512144	0.000017	–9.64
LHG-3		0.723303	0.000034	0.512153	0.000019	–9.46
ZSGR-1	34.3° N, 85.85° E	0.718328	0.000032	0.512146	0.000035	–9.6
ZSGR-2		0.718229	0.000017	0.512142	0.000035	–9.68
ZSGR-3		0.717352	0.000017	0.512127	0.000039	–9.97
DKMD	33.01° N, 92.01° E	0.713192	0.000050	0.512099	0.000025	–10.51
GL-1	33.58° N, 91.18° E	0.717546	0.000009	0.512146	0.000010	–9.60
GL-2		0.721331	0.000008	0.512152	0.000005	–9.48
GL-3		0.721786	0.000007	0.512149	0.000019	–9.54
GL-4		0.718356	0.000010	0.512115	0.000007	–10.20
GL-5		0.720991	0.000007	0.512167	0.000022	–9.19
JMYZ-1	30.21° N, 82.16° E	0.740694	0.000020	0.511907	0.000018	–14.26
JMYZ-2		0.737211	0.000034	0.511946	0.000019	–13.5
JMYZ-3		0.726710	0.000037	0.512102	0.000101	–10.46
Yala	85.62° N, 28.23° E	0.740112	0.000021	0.511834	0.000014	–15.68
QM-1	28.01° N, 86.97° E	0.728869	0.000012	0.511854	0.000011	–15.29
QM-2		0.728956	0.000007	0.511802	0.000014	–16.31
QM-3		0.728129	0.000008	0.511821	0.000012	–15.94
QM-4		0.728057	0.000007	0.511832	0.000012	–15.72
QM-5		0.730596	0.000008	0.511197	0.000021	–28.11
QM-6		0.752618	0.000014	0.511756	0.000018	–17.21
QM-7		0.757407	0.000010	0.511839	0.000007	–15.59
QM-8		0.741166	0.000011	0.511816	0.000015	–16.03
QM-9		0.743253	0.000009	0.511883	0.000015	–14.73
ZD-1	30.47° N, 90.65° E	0.719966	0.000021	0.512068	0.000040	–11.12
ZD-2		0.718285	0.000020	0.512059	0.000028	–11.29
ZD-3		0.720414	0.000022	0.512032	0.000018	–11.82
ZD-4		0.721305	0.000020	0.511977	0.000044	–12.89
DML-1	29.37° N, 97.00° E	0.729095	0.000032	0.511911	0.000016	–14.18
DML-2		0.730605	0.000018	0.511851	0.000025	–15.35
DML-3		0.730996	0.000020	NA	NA	NA
DML-4		0.735863	0.000024	0.511764	0.000019	–17.05
YL-1	27.1° N, 100.2° E	0.719881	0.000021	0.512120	0.000020	–10.1
YL-2		0.717417	0.000021	NA	NA	NA
YL-3		0.717145	0.000026	0.512055	0.000038	–11.37

China and south of Mongolia (Chen and others, 2007). The Sr–Nd isotopic composition at the TS (Tien Shan) site is similar to that of the deserts of the northern margin of the Tibetan Plateau (NM_TP; e.g. Taklimakan and Qaidam deserts) (Chen and others, 2007). Two samples, however, show relatively high $\varepsilon_{Nd}(0)$ values, suggesting possible mixing of dust sources with that from the north of China (e.g. Gurbantunggut and Gobi deserts), likely transported along with the winter monsoons (Sun and others, 2001). The Sr–Nd isotopic compositions in samples from the northern TP, including MS, LHG, DKMD, ZSGR and GL (Table 1), are highly homogeneous, and all fall within the range of NM_TP deserts (Chen and others, 2007) (Fig. 2), suggesting a similar dust source at these sites. Compared to the available dataset for TP, the $\varepsilon_{Nd}(0)$ values in ZSGR (–9.97 to –9.6) are significantly different from the TP local dust source (central Qiangtang Terrane) (–20.72 to –14.60) (Zhang and others, 2007; W. Wu and others, 2010), indicating a possible long-range transport of dust from the northern deserts.

Most Sr–Nd isotopic compositions for samples in the southern TP and the Himalaya (JMYZ, QM, Yala and DML) are close to the values of the Himalaya–India regional dataset (Fig. 2) (Tripathi and others, 2004; Najman, 2006). Note that due to very low insoluble particle concentration in the QM sample, we used the isotopic data from previous studies (Xu and others, 2009). The dust source in QM has been suggested to be a mixture of dust with a minor fraction from the northwest Indian arid region and a major fraction

https://doi.org/10.3189/2012JoG12J006 Published online by Cambridge University Press

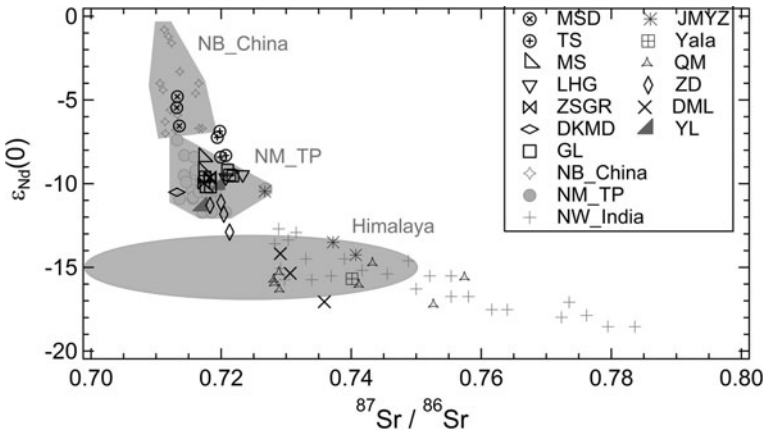

Fig. 2. The Nd vs Sr isotopic composition of insoluble particles in snow samples collected from 13 glaciers over western China. Data obtained from potential source areas in the northern boundary of China (NB_China) (Chen and others, 2007), the northern margin of TP (NM_TP) (Chen and others, 2007), the Himalaya (Najman, 2006) and the northwest Indian arid areas (NW_India) (Tripathi and others, 2004) are also shown.

from the local source (from glacial debris and exposed rock walls) (Xu and others, 2009). The Sr–Nd isotopic compositions in Yala, DML and two JMYZ samples also resemble those of QM, indicating the local source in these sites. This phenomenon can probably be explained by the fact that glacier debris can enter the glacier easily, owing to the high ablation rate and high physical–chemical weathering of the mountain (e.g. the DML (Hengduan mountains) site). The Sr–Nd isotopic composition in ZD (northern Nyainqentanglha mountain) mostly ranged near the edge of the NM_TP, and one sample was close to the Himalayan value (Fig. 2), indicating a transitional region of dust source or a mixing of dust deposition. During the sampling period at ZD, dirty layers were very noticeable and accumulated. The mode of size distribution was ~11 μm and the dust deposition rate was much higher than those at GLDD and ZSGR (two sites in the northern TP) (Xu and others, unpublished information), suggesting that the dominant sources of these sites are relatively close. Compared to the available dataset, the $\varepsilon_{Nd}(0)$ values in ZD fall into the range of samples from the Lhasa Terrane (–17.69 to –6.38), where ZD is located (Fig. 1) (Zhang and others, 2007; W. Wu and others, 2010). Owing to the large range of $\varepsilon_{Nd}(0)$ in this dataset, we cannot rule out other sources from the NM_TP or Himalaya–India region which we discuss further, based on the air-mass back trajectories, in Section 3.2.

The largest variation in Sr–Nd isotopic compositions is found in samples from JMYZ and YL, with one JMYZ sample and two YL samples falling into the isotopic range of NM_TP. The uncertainty of $^{143}Nd/^{144}Nd$ for this one JMYZ sample is 0.000051 (1σ), and the $\varepsilon_{Nd}(0)$ range is –9.46 to –11.45, still larger than that of the other two data points and close to the results for the NM_TP. The uncertainties of $^{143}Nd/^{144}Nd$ for these two YL samples are also small (0.000020 and 0.000038). These results suggest the reality for these data. The trajectories analyses (Section 3.2) also indicate that the potential dust source for JMYZ can be the NM_TP. For the YL sampling site, although it is much further away from the NM_TP and the trajectories analysis shows that >85% of the air mass comes from the local and/or nearby regions, the isotopic signatures clearly differ from those of DML, while their location and back-trajectory profiles are almost identical. DML likely had a local dust source. These results indicate that dust may have been carried to these two sites from the northern deserts via long-range transport over the TP. The estimated contribution from these dust sources is presented in Section 3.3.

3.2. Possible dust source and transport route

To facilitate identification of source regions, air-mass back trajectories (for a 3 day period, ending at each sampling site) are computed and classified using GIS-based software (TrajStat; Wang and others, 2009) with storm frequency data during the high dust-storm frequency season, March–June, in 2008 and 2009 (downloaded from the US National Oceanic and Atmospheric Administration (NOAA) gridded meteorological archives, http://www.arl.noaa.gov/ready/hysplit4.html) (Fig. 3). Overall, most clustering trajectories in the sampling sites originated from the west, reflecting the typical westerlies climate of Central Asia, while some clusters originated from the northwest at the northern sites, and others from the southwest at the southern sites.

About 60% of the trajectories at MSD originated from the west and northwest, while the rest were short trajectories from the direction of the Gobi desert (Fig. 3), supporting the similarity of Sr–Nd isotopic composition between the MSD samples and samples from the northern boundary of China and south of Mongolia. Over 70% of trajectories at TS traveled along the Taklimakan desert, while about 10% originated from the northern region of TS which covers the Gurbantungut desert. This finding agrees with the speculation, based on the isotopic data, that dust can also travel from northern arid areas. The sampling sites in the northern TP (LHG, ZSGR, DKMD and GL) show similar clustering patterns, with the majority of trajectories coming from the Taklimakan desert and the Tarim basin, which agrees with the relatively homogeneous Sr–Nd isotopic compositions of these sites. These trajectories are also consistent with results from the Cloud–Aerosol Lidar and Infrared Pathfinder Satellite Observations (CALIPSO), which show that dust primarily originated from the Taklimakan desert and the Tarim basin, traveled eastward and covered the northern slope and eastern region of the TP (Liu and others, 2008). Over 90% of the trajectories at MS originated from the west, northwest or southwest, while only 6.5% originated from the Taklimakan desert. However, it is still possible that dust at

https://doi.org/10.3189/2012JoG12J006 Published online by Cambridge University Press

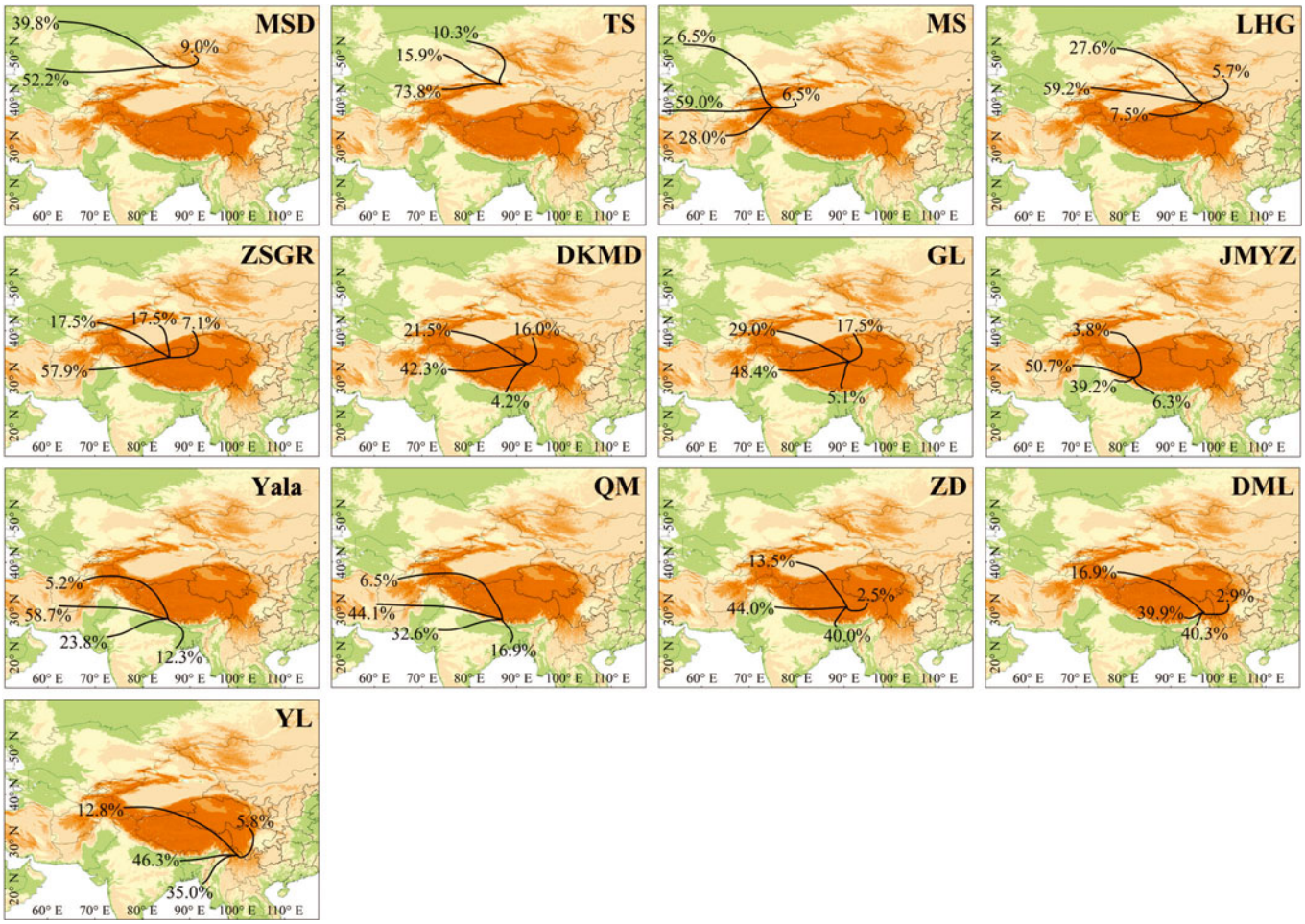

Fig. 3. Three-day backward air-mass trajectory cluster maps of each sampling site during the high-frequency dust storm season (March–June) between 2008 and 2009. The trajectories are calculated every 6 hours at 500 m above each sampling site using the TrajStat software package.

MS could be mainly from this desert due to its short distance from Taklimakan.

Most trajectories at sites in the Himalaya (JMYZ, QM and Yala) originated from the west and/or the southwest, and partly (~5%) from the north. JMYZ is close to the arid regions of northwest India, and dust can be transported along the Himalaya during the pre-monsoon as seen from aerosol results from the Nepal Himalaya (Carrico and others, 2003). The Sr–Nd isotopic data also suggest that the limited number of trajectories (~4%) originating from the northern desert were able to deliver dust to JMYZ despite the huge elevation difference (~6000 m) between the NM_TP and the Himalaya. Satellite data have demonstrated that dust layers may be lifted to altitudes of 11–12 km to the TP in the spring (Liu and others, 2008). In addition, JMYZ is the closest of these three Himalayan sampling sites to the Taklimakan desert. The dust source at QM and Yala should be similar to that of JMYZ, which shows the mixed dust signal because of the similar air-mass trajectories and identical location, but the isotopic signal from the NM_TP at these two sites is likely weakened by the low dust flux or the annual variation due to the different sampling time for these three sites.

Sampling sites in the southeast TP (ZD, DML and YL) also exhibit clustering trajectories from the west and southwest, although with relatively low speed. Meanwhile, relatively large portions of the trajectories (~15%) compare with the Himalayan sites, coming from the north with high speed. At ZD, 44% of trajectories came from the Indian arid regions and then crossed the western TP. This route can not only transport dust from Indian arid areas but also may blow up huge amounts of local dust which can be transported to the mountain areas and the surrounding cities such as Lhasa, as has been shown in published satellite images (Fang and others, 2004). The dust from northern trajectories (~14%) can also travel to ZD via the high-elevation route. From isotopic features, the dust source at ZD seems likely to be a mixture of dust sourced from the Indian arid regions, locally and from the NM_TP. At DML and YL, the clustering trajectories mainly originate from the surrounding regions with low speed except for those from the north. Liu and others (2008) suggested that dust particles traveling from the northern TP may be trapped by spiral airflows caused by the geological structure of the region, causing the northern and southern westerly jets in the southeastern TP to join. This could explain why the Sr–Nd isotopic composition in YL shows a dust signature typical of the northern TP margin. The signals of isotopic composition in DML, which did not show the dust signal of the NM_TP, were likely weakened due to high local dust deposition.

3.3. Case study of northern deserts' dust contribution to the southern sites

To estimate the contribution of dust in the northern deserts to the three southern sites, ZD, JMYZ and YL, we adopted the

https://doi.org/10.3189/2012JoG12J006 Published online by Cambridge University Press

conventional mixing equation:

$$X = \frac{(\varepsilon_{Nd}(0))_{SAMP} - (\varepsilon_{Nd}(0))_{HMAVG}}{(\varepsilon_{Nd}(0))_{NOR\_MAX} - (\varepsilon_{Nd}(0))_{HM\_AVG}}$$

where X is the fraction of contribution from the northern desert, $(\varepsilon_{Nd}(0))_{SAMP}$ is the $\varepsilon_{Nd}(0)$ value at any one of the three sampling sites, and $(\varepsilon_{Nd}(0))_{NOR\_MAX}$ (–7.4) and $(\varepsilon_{Nd}(0))_{HM\_AVG}$ (–15.78) are used as the potential end-members, and represent the maximum value of $\varepsilon_{Nd}(0)$ in the northern desert and the average value of $\varepsilon_{Nd}(0)$ in the Himalaya, respectively. The Nd isotopic data were applied to this equation due to the small influence of particle sizes on the isotopic values (Chen and others, 2007). The $(\varepsilon_{Nd}(0))_{NOR\_MAX}$ values were taken from a dataset of the NM_TP (Chen and others, 2007). The $(\varepsilon_{Nd}(0))_{HM\_AVG}$ values were from the Himalayan dataset reported by Tripathi and others (2004).

The results show that 35–56% of dust in ZD, 18–63% of dust in JMYZ and 53–68% of dust in YL were likely transported from the northern dust sources, implying that long-range and high-altitude transport might make an important contribution to dust deposition at these sites. The dust deposition flux in ZD, JMYZ and YL was 1830, 300 and 730 $\mu g\,cm^{-2}\,a^{-1}$ respectively (Xu and others, unpublished information). Thus the contributions from the northern dust source could be around 641–1025 $\mu g\,cm^{-2}\,a^{-1}$ in ZD, 54–190 $\mu g\,cm^{-2}\,a^{-1}$ in JMYZ and 384–495 $\mu g\,cm^{-2}\,a^{-1}$ in YL. These dust deposition values are lower than those of other northern sites (Xu and others, unpublished information). However, this type of transport may have significant environmental impacts on the TP, as aerosols, including dust and anthropogenic particles, can potentially regulate the climate (Lau and others, 2006).

SUMMARY

The Sr–Nd isotopic compositions dataset presented here confirms that the dust source in most mountain glaciers of western China is local and/or regional, while dust in glaciers of the Himalaya and southeast TP can be transported from the northern desert via long-range and high-altitude transport routes, which is consistent with satellite remote detection. These results provide a better understanding of the characterization of dust transport over the mountain areas of western China and are useful when interpreting the dust provenance in ice-core records from these areas.

ACKNOWLEDGEMENTS

We thank two anonymous reviewers for valuable comments and constructive suggestions. This research was supported by grants from Natural Science Foundation of China (NSFC) (40901043, 40825017 and 41171052) and the Scientific Research Foundation of the State Key Laboratory of Cryospheric Sciences (SKLCS-ZZ-2008-01). We are also grateful to many scientists, technicians, graduate students and porters for their hard work expertly carried out in the field.

REFERENCES

Biscaye PE and 6 others (1997) Asian provenance of glacial dust (stage 2) in the Greenland Ice Sheet Project 2 ice core, Summit, Greenland. *J. Geophys. Res.,* **102**(C12), 26 765–26 781 (doi: 10.1029/97JC01249)

Bory A and 6 others (2010) Multiple sources supply eolian mineral dust to the Atlantic sector of coastal Antarctica: evidence from recent snow layers at the top of Berkner Island ice sheet. *Earth Planet. Sci. Lett.,* **291**(1–4), 138–148 (doi: 10.1016/j.epsl.2010.01.006)

Carrico CM, Bergin MH, Shrestha AB, Dibb JE, Gomes L and Harris JM (2003) The importance of carbon and mineral dust to seasonal aerosol properties in the Nepal Himalaya. *Atmos. Environ.,* **37**(20), 2811–2824 (doi: 10.1016/S1352-2310(03)00197-3)

Chen J and 7 others (2007) Nd and Sr isotopic characteristics of Chinese deserts: implications for the provenances of Asian dust. *Geochim. Cosmochim. Acta,* **71**(15), 3904–3914 (doi: 10.1016/j.gca.2007.04.033)

Duce RA, Unni CK, Ray J, Prospero JM and Merrill JT (1980) Long-range atmospheric transport of soil dust from Asia to the tropical North Pacific: temporal variability. *Science,* **209**(4464), 1522–1524 (doi: 10.1126/science.209.4464.1522)

Fang X, Han Y, Ma J, Song L, Yang S and Zhang X (2004) Dust storms and loess accumulation on the Tibetan Plateau: a case study of dust event on 4 March 2003 in Lhasa. *Chinese Sci. Bull.,* **49**(9), 953–960

Fitzgerald WF (1999) Clean hands, dirty hands: Clair Patterson and the aquatic biogeochemistry of mercury. In Davison CI ed. *Clean hands: Clair Patterson's crusade against environmental lead contamination.* Nova Science, Commack, NY, 119–137

Fujita K (2007) Effect of dust event timing on glacier runoff: sensitivity analysis for a Tibetan glacier. *Hydrol. Process.,* **21**(21), 2892–2896 (doi: 10.1002/hyp.6504)

Grousset FE and Biscaye PE (2005) Tracing dust sources and transport patterns using Sr, Nd and Pb isotopes. *Chemical Geol.,* **222**(3–4), 149–167 (doi: 10.1016/j.chemgeo.2005.05.006)

Hong S and 8 others (2009) An 800-year record of atmospheric As, Mo, Sn, and Sb in Central Asia in high-altitude ice cores from Mt. Qomolangma (Everest), Himalayas. *Environ. Sci. Technol.,* **43**(21), 8060–8065 (doi: 10.1021/es901685u)

Huang J and 6 others (2010) Dust aerosol effect on semi-arid climate over Northwest China detected from A-Train satellite measurements. *Atmos. Chem. Phys.,* **10**(14), 6863–6872 (doi: 10.5194/acp-10-6863-2010)

Kaspari S and 6 others (2011) Recent increase in black carbon concentrations from a Mt. Everest ice core spanning 1860–2000 AD. *Geophys. Res. Lett.,* **38**(4), L04703 (doi: 10.1029/2010GL046096)

Lau KM, Kim MK and Kim KM (2006) Asian summer monsoon anomalies induced by aerosol direct forcing: the role of the Tibetan Plateau. *Climate Dyn.,* **26**(7–8), 855–864 (doi: 10.1007/s00382-006-0114-z)

Liu Z and 10 others (2008) Airborne dust distributions over the Tibetan Plateau and surrounding areas derived from the first year of CALIPSO lidar observations. *Atmos. Chem. Phys.,* **8**(16), 5045–5060 (doi: 10.5194/acp-8-5045-2008)

Najman Y (2006) The detrital record of orogenesis: a review of approaches and techniques used in the Himalayan sedimentary basins. *Earth-Sci. Rev.,* **74**(1–2), 1–72 (doi: 10.1016/j.earscirev.2005.04.004)

Sun J, Zhang M and Liu T (2001) Spatial and temporal characteristics of dust storms in China and its surrounding regions, 1960–1999: relations to source area and climate. *J. Geophys. Res.,* **106**(D10), 10 325–10 333 (doi: 10.1029/2000JD900665)

Thompson LG, Yao T, Mosley-Thompson E, Davis ME, Henderson KA and Lin P (2000) A high-resolution millennial record of the south Asian monsoon from Himalayan ice cores. *Science,* **289**(5486), 1916–1919 (doi: 10.1126/science.289.5486.1916)

Tripathi JK, Bock B, Rajamani V and Eisenhauer A (2004) Is River Ghaggar, Saraswati? Geochemical constraints. *Current Sci.,* **87**(8), 1141–1144

Wang YQ, Zhang XY and Draxler RP (2009) TrajStat: GIS-based software that uses various trajectory statistical analysis methods to identify potential sources from long-term air pollution

https://doi.org/10.3189/2012JoG12J006 Published online by Cambridge University Press

measurement data. *Environ. Model. Softw.,* **24**(8), 938–939 (doi: 10.1016/j.envsoft.2009.01.004)

Wu G, Zhang C, Zhang X, Tian L and Yao T (2010) Sr and Nd isotopic composition of dust in Dunde ice core, Northern China: implications for source tracing and use as an analogue of long-range transported Asian dust. *Earth Planet. Sci. Lett.,* **299**(3–4), 409–416 (doi: 10.1016/j.epsl.2010.09.021)

Wu W, Xu S, Yang J, Yin H, Lu H and Zhang K (2010) Isotopic characteristics of river sediments on the Tibetan Plateau. *Chemical Geol.,* **269**(3–4), 406–413 (doi: 10.1016/j.chemgeo.2009.10.015)

Xu J, Hou S, Qin D, Kang S, Ren J and Ming J (2007) Dust storm activity over the Tibetan Plateau recorded by a shallow ice core from the north slope of Mt. Qomolangma (Everest), Tibet-Himal region. *Geophys. Res. Lett.,* **34**(17), L17504 (doi: 10.1029/2007GL030853)

Xu J, Hou S, Chen F, Ren J and Qin D (2009) Tracing the sources of particles in the East Rongbuk ice core from Mt. Qomolangma. *Chinese Sci. Bull.,* **54**(10), 1781–1785

Zhang K-J, Zhang Y-X, Li B and Zhong L-F (2007) Nd isotopes of siliciclastic rocks from Tibet, western China: constraints on provenance and pre-Cenozoic tectonic evolution. *Earth Planet. Sci. Lett.,* **256**(3–4), 604–616 (doi: 10.1016/j.epsl.2007.02.014)

Zhang Q and 8 others (2012) Mercury distribution and deposition in glacier snow over western China. *Environ. Sci. Technol.,* **46**(19), 5404–5413

MS received 14 January 2012 and accepted in revised form 25 May 2012